

See discussions, stats, and author profiles for this publication at: <https://www.researchgate.net/publication/8921516>

Direct Analysis of Oxidizing Agents in Aqueous Solution with Attenuated Total Reflectance Mid-Infrared Spectroscopy and Diamond-like Carbon Protected Waveguides

ARTICLE in ANALYTICAL CHEMISTRY · FEBRUARY 2004

Impact Factor: 5.64 · DOI: 10.1021/ac034699d · Source: PubMed

CITATIONS

27

READS

87

8 AUTHORS, INCLUDING:



Markus Janotta

Georgia Institute of Technology

13 PUBLICATIONS 281 CITATIONS

SEE PROFILE



W. Waldhauser

Joanneum Research Forschungsgesellschaft ...

91 PUBLICATIONS 693 CITATIONS

SEE PROFILE



Juergen M Lackner

Joanneum Research Forschungsgesellschaft ...

116 PUBLICATIONS 723 CITATIONS

SEE PROFILE



Boris Mizaikoff

Universität Ulm

310 PUBLICATIONS 4,799 CITATIONS

SEE PROFILE

Direct Analysis of Oxidizing Agents in Aqueous Solution with Attenuated Total Reflectance Mid-Infrared Spectroscopy and Diamond-like Carbon Protected Waveguides

Markus Janotta,[†] Frank Vogt,[†] Hannes-Stefan Voraberger,^{*,‡} Wolfgang Waldhauser,^{*,§} Jürgen M. Lackner,[§] Christoph Stotter,[§] Michael Beutl,^{||} and Boris Mizaikoff^{*,†}

School of Chemistry and Biochemistry, Georgia Institute of Technology, Atlanta, Georgia 30332-0400, Institute of Chemical Process Development and Control, Joanneum Research, Steyrergasse 17, 8010 Graz, Austria, Laser Center Leoben, Joanneum Research, Leobner Strasse 94, A-8712 Niklasdorf, Austria, and Institute of Nanostructured Materials and Photonics, Joanneum Research, Franz-Pichler-Strasse 30, A-8160 Weiz, Austria

A novel approach for the direct detection of oxidizing agents in aqueous solution is presented using diamond-like carbon (DLC) protected waveguides in combination with attenuated total reflectance (ATR) mid-infrared spectroscopy. Pulsed laser deposition was applied to produce high-quality DLC thin films on ZnSe ATR crystals with thicknesses of a few 100 nm. Scanning electron microscopy and X-ray photoelectron spectroscopy has been used to investigate the surface properties of the DLC films including the sp^3/sp^2 hybridization ratio of the carbon bonds. Beside excellent adhesion of the DLC coatings to ZnSe crystals, these films show high chemical stability against strongly oxidizing agents. IR microscopy was utilized to compare differences in the chemical surface modification of bare and protected ATR waveguides when exposed to hydrogen peroxide, peracetic acid, and peroxydisulfuric acid. The feasibility of DLC protected waveguides for real-time concentration monitoring of these oxidizing agents was demonstrated by measuring calibration sets in a concentration range of 0.2–10%. Additionally, principal component regression has been applied to analyze multicomponent mixtures of hydrogen peroxide, acetic acid, and peracetic acid in aqueous solution. Due to high chemical stability and accurate monitoring capabilities, DLC protected waveguides represent a novel approach for directly detecting oxidizing agents in aqueous solution with promising potential for industrial process analysis.

numerous applications in the wastewater and textile treatment, sterilization (clean-in-place), and chemical industry. For instance, strongly oxidizing compounds such as hydrogen peroxide (HP) and peracetic acid (PAA) are increasingly used as they represent a viable alternative with higher oxidation potential to many of the routinely applied halogenated compounds. Additionally, improvements for safer and more efficient storage of peroxides (e.g., stabilization with phosphates and tin(IV) materials via hydrocolloid formation) have promoted their industrial application.¹ While typical concentration ranges for oxidizing agents applied in the food and beverage industries are between 50 and 1000 ppm, sensing systems applied in peroxide on-line monitoring for the paper bleaching industry frequently encounter concentrations of up to 10%.² Resulting, in situ analytical techniques, which monitor oxidant concentration levels on-line, demand sensor systems with superior long-term stability operable at such harsh measurement conditions.

Reliable determination of HP and PAA is routinely performed by titration techniques utilizing compound-specific differences of redox properties.³ Aside from these discontinuous methods, hydrogen peroxide detection is performed by spectroscopic determination utilizing changes in color,⁴ fluorescence,⁵ or chemiluminescence.^{6,7} Electrochemical methods for the determination of hydrogen peroxide can be divided into amperometric,⁸ potentiometric,⁹ and conductometric methods.¹⁰ In particular, amperometric sensors offer the possibility of direct on-line monitoring. Due to the required overpotential noble metal electrodes, such

Over the past decades, interest for on-line monitoring of chemically aggressive agents has grown significantly due to

* Corresponding authors: (e-mail) boris.mizaikoff@chemistry.gatech.edu, (phone) +1-404-894-4030; (fax) +1-404-894-7452, (information) <http://asl.chemistry.gatech.edu>; (e-mail) hannes.voraberger@joanneum.at, (phone) +43-316-876-1228, (fax) +43-316-8769-1228, (information) <http://www.joanneum.at>; (e-mail) wolfgang.waldhauser@joanneum.at, (phone) +43-316-876-2311, (fax) +43-316-8769-2311, (information) <http://www.joanneum.at>.

[†] Georgia Institute of Technology.

[‡] Institute of Chemical Process Development and Control, Joanneum Research.

[§] Laser Center Leoben, Joanneum Research.

^{||} Institute of Nanostructured Materials and Photonics, Joanneum Research.

- (1) Jones, C. W. *Applications of Hydrogen Peroxide and Derivatives*; Royal Society of Chemistry: Cambridge, 1999; p 72.
- (2) Temmerman, E.; Westbroek, P. Int. Pat. Appl. WO1996023215, 1996.
- (3) Greenspan, F. P.; McKellar, D. G. *Anal. Chem.* **1948**, *20*, 1061–1063.
- (4) Clapp, P. A.; Evans, D. F. *Anal. Chim. Acta* **1991**, *243* (2), 217–220.
- (5) Lobnik, A.; Čajlaković, M. *Sens. Actuators, B* **2001**, *74*, 194–199.
- (6) Price, D.; Worsfold, P. J.; Mantoura, R. F. C. *Anal. Chim. Acta* **1994**, *298* (1), 121–128.
- (7) Diaz, A. N.; Peinado, M. C. R.; Minguez, M. C. T. *Anal. Chim. Acta* **1998**, *363* (2–3), 221–227.
- (8) Westbroek, P.; Van Haute, P.; Temmerman, E. *Fresenius' J. Anal. Chem.* **1996**, *354* (4), 405–409.
- (9) Ravensbergen, D. W. PCT Int. Appl. 9118296 A1, 1991.
- (10) Tay, B. T.; Tat, K. P.; Gunasingham, H. *Analyst* **1988**, *113* (4), 617–620.

as gold or platinum and metallized carbons,^{11,12} have been applied reducing the overpotential. In addition, biosensing approaches have been reported based on horseradish peroxidase.¹³ However, while this strategy enables low operating potentials, issues such as electrode fouling and enzyme stability are not yet solved, when applying the sensor system for long-term concentration monitoring.

Peracetic acid is technically prepared from acetic acid and hydrogen peroxide in the presence of an acidic catalyst, typically H₂SO₄.¹⁴ Several analytical techniques for the determination of PAA including photometry,¹⁵ spectrophotometry,¹⁶ electrochemical sensing,¹⁷ and gas chromatography¹⁸ have been reported. In addition, simultaneous determination techniques for HP and PAA have successfully been demonstrated using HPLC,¹⁹ electroanalysis²⁰ and via selective photometric determination of PAA in the presence of hydrogen peroxide.²¹

Mid-infrared (MIR) spectroscopy is recognized as an analytical technique of persistently increasing importance. Continuous progress in development of MIR-transparent optical waveguides enables the extension of conventional IR spectroscopy toward spectroscopic sensing systems.^{22,23} Taking advantage of molecule-specific vibrational and rotational transitions and their resulting distinctive absorption patterns in the MIR spectral range, the development of compact sensor systems for selective multicomponent analysis is enabled.^{26,27} While diamond is a robust material suitable for IR spectroscopy,²⁸ the most commonly applied attenuated total reflectance (ATR) waveguide materials with sufficient transparency in the spectral region of approximately 3–15 μm are germanium, thallium bromides (e.g., KRS-5), and zinc selenide. However, most of these materials are susceptible to strong acids, bases, and oxidizing agents. Consequently, the majority of spectroscopic sensing systems rely on waveguide surface protection via polymer-based membranes. This approach additionally increases selectivity and sensitivity with the coating serving as solid-phase extraction membrane for the analytes of interest, while simultaneously excluding water from interaction with the evanescent field. Although this sensing method is well-established, it suffers from disadvantages such as diffusion-controlled sensor

response time.^{29–31} In contrast, sensors based on direct interaction of analytes with the evanescent field are prone to chemical interferences and chemical degradation of the waveguide. Hence, they are limited in application to dedicated analytical problems in well-defined matrixes and to considerably high analyte concentration levels in the milligram per liter range.³²

Recently, research in amorphous hydrogenated carbon films has been significantly promoted due to numerous unique properties including high level of hardness (up to 80 GPa), high resistivity (up to $10^{16} \Omega \text{ cm}^{-1}$), transparency over a wide optical range (optical band 1.0–4.0 eV), and chemical stability.³³ Diamond-like carbon (DLC) is an important form of amorphous carbon composed of a mixture of sp³- and sp²-coordinated carbon. The beneficial properties of DLC derive from the sp³ constituents making DLC mechanically robust, transparent in the infrared spectral range, and chemically inert.³⁴ Besides the well-established methods of ion-plasma deposition, pulsed laser deposition (PLD) is particularly suitable for producing high-quality DLC films.³⁵ Due to their numerous advantages, DLC coatings have found applications as hard protective coatings for magnetic disk drives, antireflective coatings for IR windows, and field emission source for emitters.³⁴

The focus of this study is to demonstrate for the first time the feasibility of DLC protected mid-IR waveguides for real-time concentration monitoring of strongly oxidizing agents with the potential of continuous monitoring applications in the paper bleaching industry or during wastewater treatment. The feasibility of this system has been tested for hydrogen peroxide, peracetic acid, and peroxydisulfuric acid as target analytes. Thorough studies of the DLC thin-film structure and properties including sp³/sp² hybridization ratio of the carbon bonds are presented. Chemical and mechanical stability of the protective DLC layer against oxidizing agents and remaining transparency of DLC-coated zinc selenide ATR waveguides were analyzed. Calibration experiments demonstrate the suitability of ATR measurements for reliable quantitative detection of the investigated analytes. Dynamic experiments following concentration changes demonstrate the on-line monitoring capabilities of the developed approach. Finally, principal component regression (PCR)^{36–38} has successfully been applied for multicomponent analysis of mixtures of hydrogen peroxide, acetic acid, and peracetic acid in aqueous solution.

EXPERIMENTAL SECTION

Chemicals. Hydrogen peroxide (30 wt % solution in water), peroxydisulfuric acid, acetic acid and peracetic acid (32 wt % solution in dilute acetic acid) were purchased from Aldrich

- (11) Newman, J. D.; White, S. F.; Tothill, I. E.; Turner, A. P. F. *Anal. Chem.* **1995**, *67*, 4594–4599.
- (12) Sampath, S.; Lev, O. J. *Electroanal. Chem.* **1997**, *426* (1–2), 131–137.
- (13) Moody, A.; Setford, S.; Saini, S. *Analyst* **2001**, *126* (10), 1733–1739.
- (14) Boullion, G.; Lick, C.; Schank, K. In *The Chemistry of Peroxides*; Patai, S., Ed.; John Wiley & Sons: London, 1983; pp 287–298.
- (15) Binder, W. H.; Menger, F. M. *Anal. Lett.* **2000**, *33* (3), 479–488.
- (16) Fischer, W.; Arlt, E.; Brabänder, B. Merck Patent GmbH. U.S. 4 900 682, 1988.
- (17) McVey, I. F.; Desantis, B. J.; Lewandowski, J. J.; Thomas, K. L.; Schindly, B. *E PCT Int. Appl.* 2001.
- (18) Cairns, G. T.; Diaz, R. R.; Selby, K.; Waddington, D. J. *Chromatogr.* **1975**, *103*, 381–384.
- (19) Pinkernell, U.; Effkemann, S.; Karst, U. *Anal. Chem.* **1997**, *69*, 3623–3627.
- (20) Awad, M. I.; Oritani, T.; Ohsaka, T. *Anal. Chem.* **2003**, *75*, 2688–2693.
- (21) Pinkernell, U.; Lüke, H.-J.; Karst, U. *Analyst* **1997**, *122* (6), 567–571.
- (22) Saito, M.; Kikuchi, K. *Opt. Rev.* **1997**, *4* (5), 527–538.
- (23) Lendl, B.; Mizaikoff, B. In *Handbook of Vibrational Spectroscopy*; Chalmers, J. M., Griffiths, P. R., Eds.; John Wiley: New York, 2002; Vol. 2, pp 1541.
- (24) Heise, H. M.; Kupper, L.; Butvina, L. N. *Anal. Bioanal. Chem.* **2003**, *375* (8), 1116–1123.
- (25) Mizaikoff, B. *Water Sci. Technol.* **2003**, *47* (2), 35–42.
- (26) Mizaikoff, B. *Meas. Sci. Technol.* **1999**, *10*, 1185–1194.
- (27) Vogt, F.; Kraft, M.; Mizaikoff, B. *Appl. Spectrosc.* **2002**, *56* (10), 1376–1380.
- (28) Coates, J.; Sanders, A. *Spectrosc. Eur.* **2000**, *12* (5), 12–22.

- (29) Jakusch, M.; Janotta, M.; Mizaikoff, B.; Mosbach, K.; Haupt, K. *Anal. Chem.* **1999**, *71*, 4786–4791.
- (30) Mizaikoff, B.; Lendl, B. In *Handbook of Vibrational Spectroscopy*; Chalmers, J. M., Griffiths, P. R., Eds.; John Wiley: New York, 2002; Vol. 2, p 1560.
- (31) Mizaikoff, B. *Anal. Chem.* **2003**, *75*, 258A–267A.
- (32) Jeona, J. S.; Raghavana, S.; Sperline, R. P. *Colloids Surf., A* **1994**, *92*, 255–265.
- (33) Wei, Q.; Narayan, J. *Int. Mater. Rev.* **2000**, *45* (4), 133–164.
- (34) Robertson, J. *Mater. Sci. Eng.* **2002**, *R37*, 129–281.
- (35) Wei, Q.; Sankar, J.; Narayan, J. *Surf. Coat. Technol.* **2001**, *146–147*, 250–257.
- (36) Marbach, R.; Heise, M. *Chemom. Intell. Lab. Syst.* **1990**, *9*, 45–63.
- (37) Martens, H.; Næs, T. *Multivariate Calibration*, 2nd ed.; John Wiley & Sons: New York, 1991.
- (38) Egan, W.; Brewer, W.; Morgan, W. *Appl. Spectrosc.* **1999**, *53*, 218–225.

(Milwaukee, WI). Deionized water for dilution of the stock solutions was used throughout the experiments.

Preparation Diamond-like Carbon Films. The DLC coatings were fabricated by pulsed laser deposition using a homemade laboratory PLD coating system. An electrographite target (99.5% carbon, impurities of vanadium, titanium, hydrogen, and oxygen) was used for the ablation of carbon applying a pulsed Nd:YAG laser, which provides a beam with a wavelength of 1064 nm, a pulse energy of 1 J, and a pulse duration of 10 ns at a repetition rate of 10 Hz.³⁹ The target was rotated during laser irradiation, avoiding the formation of deep craters at the surface of the ATR crystal and to prevent ablation of droplets. The emitted species were deposited at room temperature ($\sim 25^\circ\text{C}$) in argon atmosphere onto ZnSe ATR elements ($50 \times 20 \times 2$ mm, 45° , Macrooptica Ltd., Moscow, Russia). Prior to film deposition, the substrates were cleaned in pure ethanol and dried with pure nitrogen. The film thickness was adjusted by varying the deposition time.

Film Characterization. The surface quality and growth structures of the DLC coatings were inspected with light microscopy and scanning electron microscopy (SEM; Cambridge Instruments Stereoscan 360).

X-ray photoelectron spectroscopy (XPS) was used to investigate the nature of chemical bonding in the coatings using an Omicron Multiprobe system with a monochromized Al K α (1486.6 eV) X-ray beam and an EA 125 energy analyzer. The spectrometer was operated in fixed analyzer energy transmission mode at a base pressure of 4×10^{-9} Pa. The resolution of the selected setup is better than 0.6 eV; the detection sensitivity is ~ 1 vol %. A sputter gun using Ar $^+$ ions was applied for cleaning the samples prior to investigation.

Attenuated Total Reflectance Spectroscopy. IR radiation coupled into the ATR waveguide incident at the crystal/water interface at angles larger than the critical angle creates an evanescent field guided along that interface. Analyte molecules in the vicinity of the waveguide absorb energy from the evanescently guided radiation at wavelengths in resonance with molecule-specific vibrational transitions. Signal detection and processing are achieved by Fourier transform infrared (FT-IR) analysis.⁴⁰

All measurements were performed with a Bruker IFS66 FT-IR spectrometer (Bruker Optics, Billerica, MA) equipped with a LN $_2$ -cooled mercury–cadmium–telluride (MCT) detector (Infrared Associates, Stuart, FL). A total of 100 scans was averaged for each spectrum at a spectral resolution of 4 cm^{-1} . For attenuated total reflectance measurements, a vertical ATR accessory (Specac Inc. Smyrna, GA) in combination with trapezoidal, DLC-coated ZnSe ATR elements was used. To prevent chemical attack of the ATR flow cell assembly by the oxidizing agents, a flow cell made from plexiglass with dimensions of $40 \times 15 \times 5$ mm was developed. A Viton O-ring placed between the plexiglass channel and the ATR crystal seals off the cell, creating a sample volume of 0.5 mL. A peristaltic pump (C8-Midi, Watson-Marlowe Alitea, Sweden) assured a constant flow rate of aqueous analyte solution through the flow cell at 3 mL/min.

Prior to sample measurements, deionized water was pumped through the cell until no significant changes in the water

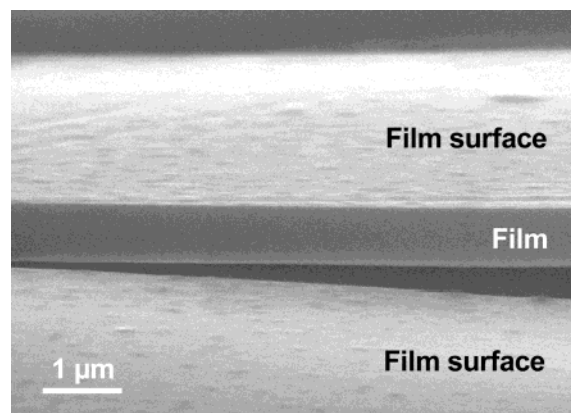


Figure 1. SEM micrograph of a fracture section of DLC film indicating a dense film structure and a smooth film surface.

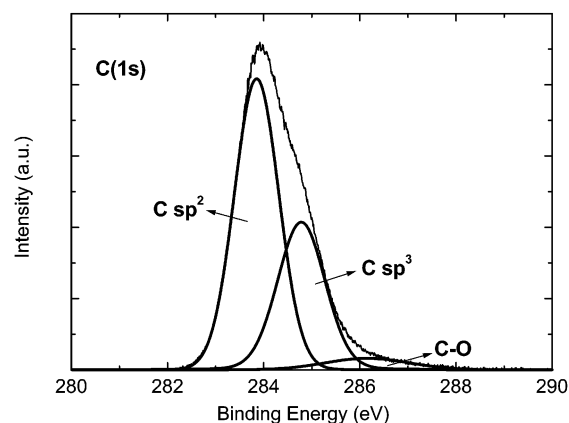


Figure 2. XPS spectra of the C(1s) peak of a DLC film and the deconvolution of the measured cumulative peak and the sp², sp³, and C–O peaks, each being a mixture of a Gaussian and Lorentzian peak.

absorption bands occurred and a background spectrum was recorded. Sample solutions with increasing analyte concentration were measured by collecting spectra in intervals of 30 s for a period of up to 5 min.

RESULTS AND DISCUSSION

Preliminary experiments have shown that strongly oxidizing agents such as peracetic acid immediately chemically degrade ZnSe crystals due to formation of H $_2$ Se. H $_2$ Se is subsequently oxidized by hydrogen peroxide or peracetic acid to reddish Se, which has been observed at the surface of unprotected PAA-treated ZnSe ATR crystals. As this degradation significantly reduces the optical throughput of the waveguide, appropriate protective surface layers are a basic necessity. DLC films deposited onto ZnSe waveguides with a maximum thickness of 200 nm provide the required chemical and mechanical stability against oxidizing agents, while maintaining the optical transmission properties of the waveguide in the required spectral window.

Structure and Properties of the DLC Coatings. Figure 1 shows a typical SEM micrograph of a cross-fracture section of a DLC coating with a thickness of $\sim 1\text{ }\mu\text{m}$ deposited onto a steel substrate. Besides the dense coating structure, a very smooth surface with only a few defects (e.g., larger particulates ablated from the target) can be observed. X-ray diffraction investigations indicate an amorphous film structure. XPS investigations of the

(39) Lackner, J. M.; Stotter, Ch.; Waldhauser, W.; Ebner, R.; Lenz, W.; Beutl, M. *Surf. Coat. Technol.* **2003**, 174–175, 402–407.

(40) Fahrenfort, J. *Spectrochim. Acta* **1961**, 17, 698–709.

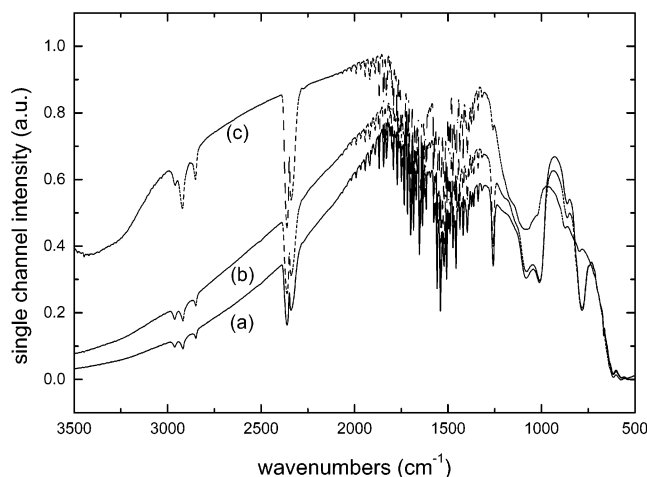


Figure 3. Single-beam spectra of ZnSe crystals coated with (a) 200- and (b) 100-nm DLC thick films in comparison to a single-beam spectra of a (c) bare ZnSe crystal.

C(1s) peak lead to a sp^3 carbon bond content of $\sim 36\%$. These values were evaluated by fitting the C(1s) peak with the two main components, diamond represented by sp^3 bonding (peak at 285.2

eV) and graphite represented by sp^2 bonding (peak at 284.4 eV), and by calculating the area fractions beneath the peaks.⁴¹ Furthermore, small contents of C–O bonds were detected. The contribution of the background was approximated by the Shirley method.⁴² The XPS spectra of the film and the deconvolution into contents corresponding to diamond and graphite, respectively, are shown in Figure 2. The relatively low sp^3 content of the coating is in agreement with previously reported findings by Voevodin and Donely⁴³ on the growth of mainly graphitic films produced by PLD of carbon when employing 1064-nm Nd:YAG laser radiation at laser pulse power densities lower than 10^{11} W cm⁻².

Investigation and Application of DLC-Coated ZnSe Waveguides. Crucial parameters for any type of protective layer deposited at the surface of MIR waveguides include the following: (i) the material should have a suitable spectral window in the wavelength region of interest, (ii) a minimum of spectrally interfering IR absorptions reducing optical radiation losses within the waveguide, and (iii) chemically protective properties at film thicknesses of <200 nm, which still enables sufficient penetration of the evanescent field into the adjacent medium. Usually, hydrophobic organic polymers with a layer thickness in the range of $1\text{--}10\text{ }\mu\text{m}$ are applied as coating materials, as they exclude water

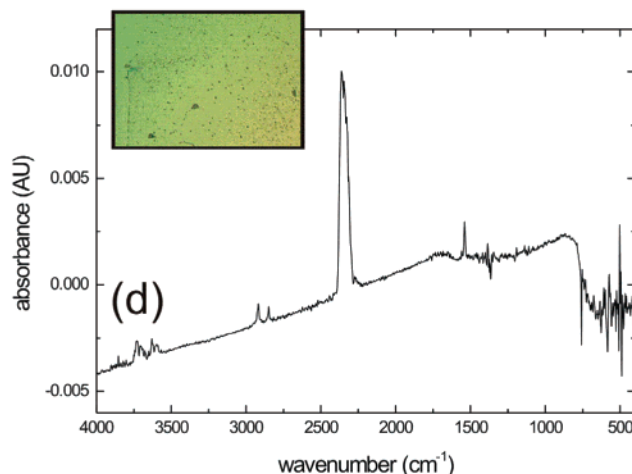
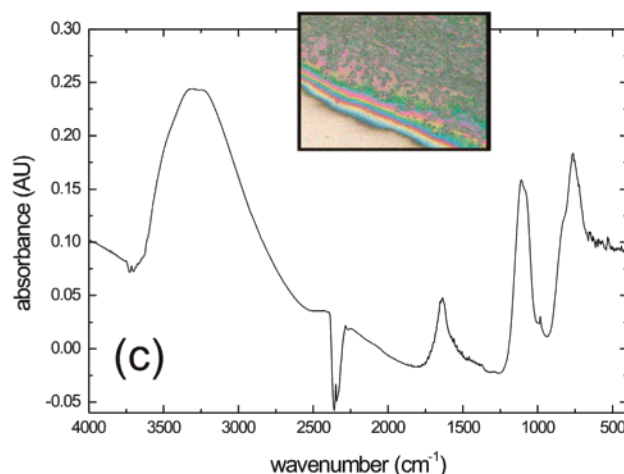
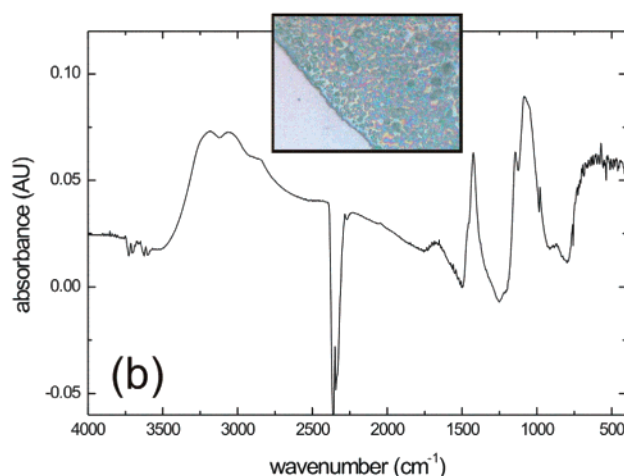
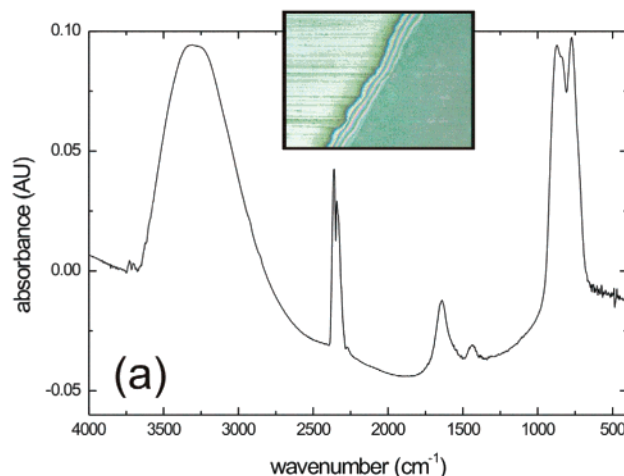


Figure 4. Optical and IR microscopic images of (a) bare ZnSe crystal treated with hydrogen peroxide, (b) bare ZnSe crystal treated with peroxydisulfuric acid, (c) bare ZnSe crystal treated with peracetic acid, and (d) 100-nm-thick DLC-coated ZnSe crystal treated with peracetic acid (resolution optimum images: $100\times$ magnification; parameters for IR-Mic images, transmission mode; spectral resolution, 4 cm^{-1} ; spot size, $1 \times 1\text{ mm}$; 30 min of exposure time when applying the oxidizing agents to the ZnSe crystal).

being a strong IR absorber from the analytical volume probed by the evanescent field. In contrast, this study is focused on highly inert, thin layers of diamond-like carbon deposited onto the surface of ZnSe crystals for direct determination of oxidizing agents in aqueous solution at concentrations of $>0.1\%$ (v). These films should demonstrate sufficient mechanical and chemical stability combined with rapid sensor response. In Figure 3, single-beam spectra of a bare (c) ZnSe waveguide and crystals coated with either 100- (b) or 200-nm (a) DLC layers are shown. As expected, deposition of a thicker DLC film results in reduced transmission though even a 200-nm film still provides sufficient energy throughput for quantitative detection in the percentage concentration range. In particular, the provided spectral window in the wavelength region from 3000 to 600 cm^{-1} with the low-frequency cutoff determined by the MCT detector is of interest for practical applications as MIR detection of various classes of strongly oxidizing analytes is enabled. However, due to the absence of nonpolar recognition membranes and increasing absorption features of the DLC layer above 2700 cm^{-1} , quantification of lower concentrated compounds will be limited. Absorption features evident around 2900 cm^{-1} (C–H stretching vibrations) and in the fingerprint region of the single-beam spectra are attributed to the absorbance of the sealing polymers that are in contact with the waveguide surface, i.e., a Teflon ring avoiding mechanical damage of the crystal by the plexiglass cell and a Viton ring creating the sample compartment for flow cell experiments.

Mechanical stability studies concerning wear and friction forces demonstrated sufficient adhesion of the DLC membranes to the ATR waveguides. Small droplets of peracetic acid were applied to a ZnSe/DLC interface, and within a few minutes, formation of reddish Se as oxidation product was observed at the uncoated sections, while parts of the crystal, which were still coated with the protective layer, remained resistant. Consequently, effects of oxidizing agents were studied more extensively on ZnSe crystal surfaces with unprotected and coated sections covered with a 100-nm DLC layer, respectively. Interface regions were exposed to various strongly oxidizing agents, including hydrogen peroxide, peracetic acid, and peroxydisulfuric acid. Optical microscopy images and IR-microscopic data (a–d) were recorded at the treated surface sections of the crystals and are summarized in Figure 4. Compared to the DLC-coated crystal, the unprotected waveguide exhibits severe surface modifications independent from the type of oxidant, which is particularly evident in the interface region between the undamaged surface (lower left corner of images in Figure 4) and the chemically attacked section. Microscopic images of freshly prepared DLC-coated waveguides were compared to images of DLC-coated waveguides after the chemical stability studies, resulting in no visible alteration of the surface. To further corroborate the indicated inertness of DLC protected crystals, localized spectra measured by IR microscopy of areas exposed to oxidizing agents during the chemical stability experiments were analyzed. Either an unmodified ZnSe crystal surface or a freshly prepared DLC-coated surface has been used as background spectrum. Except for the characteristic CO_2 stretching vibration around 2350 cm^{-1} , which is due to uncompensated atmospheric CO_2 , the absorbance spectrum of the DLC-coated

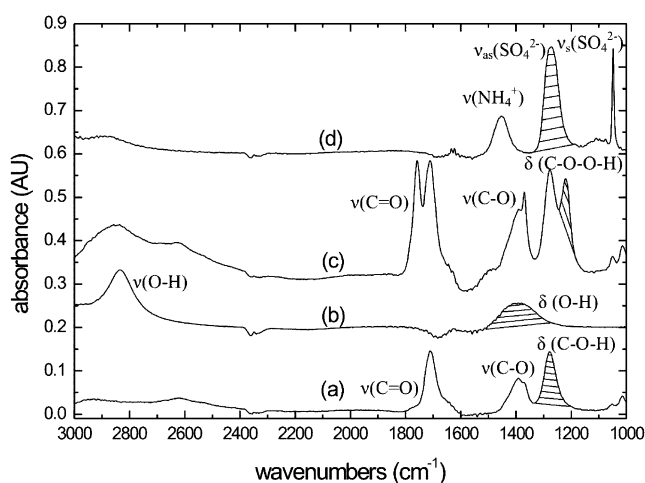


Figure 5. IR absorbance spectra of aqueous analyte solution (5% v/v) of (a) acetic acid, (b) hydrogen peroxide, (c) peracetic acid, and (d) peroxydisulfuric acid (water absorbance compensated via reference spectrum).

Table 1. Analyte-Specific Vibrational IR Features of (a) Acetic Acid, (b) Hydrogen Peroxide, (c) Peracetic Acid, and (d) Peroxydisulfuric Acid

	label	peak position (cm^{-1})	type of vibration
acetic acid	A1	1710	$\nu(\text{C}=\text{O})$
	A2	1390	$\nu(\text{C}-\text{O})$
	A3	1276	$\delta(\text{C}-\text{O}-\text{H})$
hydrogen peroxide	H1	2832	$\nu(\text{O}-\text{H})$
	H2	1382	$\delta(\text{O}-\text{H})$
peracetic acid	P1	1758, 1712	$\nu(\text{C}=\text{O})$
	P2	1390	$\nu(\text{C}-\text{O})$
	P3	1276, 1217	$\delta(\text{C}-\text{O}-\text{O})$
peroxydisulfuric acid	S1	1452	$\nu(\text{NH}_4^+)$
	S2	1272	$\nu_{\text{as}}(\text{O}-\text{SO}_3^{2-})$
	S3	1048	$\nu_{\text{s}}(\text{O}-\text{SO}_3^{2-})$

crystal surface remains constant before and after oxidant treatment. This indicates that no chemical modification has occurred (d). In contrast, each oxidizing agent can be identified by several characteristic absorption bands after treatment of the uncoated crystal sections. In the case of hydrogen peroxide (b) and peracetic acid (c), O–H stretching and deformation vibrations are evident, which gives reason to believe that during the oxidation process $\text{Zn}(\text{OH})_2$ is formed at the surface. Treatment with peroxydisulfuric acid provides less pronounced O–H vibrations with residual NH_4^+ present characterized by absorptions around 1400 cm^{-1} . This reaction seems to be supported by the appearance of a strong $\text{O}-\text{SO}_3^{2-}$ vibrational mode at 1100 cm^{-1} , which indicates formation of ZnSO_4 .

As the application of DLC protected waveguides for the detection of strongly oxidizing agents is envisaged, IR spectra of the investigated analytes hydrogen peroxide (b), peracetic acid (c), and peroxydisulfuric acid (d) are presented in Figure 5. In addition, the spectrum of acetic acid (a) is shown since aqueous peracetic acid solutions usually consist of 32% peracetic acid, 40–45% acetic acid, and $\sim 6\%$ H_2O_2 . The main IR absorption features are labeled and summarized in Table 1. Since peracetic acid is only stable in equilibrium with acetic acid and hydrogen peroxide, the respective absorbance spectrum is actually a superposition of three spectra. In addition to compound-specific spectral features

(41) Merel, P.; Tabbal, M.; Chaker, M. *Appl. Surf. Sci.* **1998**, *136*, 105–110.

(42) Tougaard, S.; Jansson, C. *Surf. Interface Anal.* **1992**, *19* (1–12), 171–174.

(43) Voevodin, A. A.; Donley, M. S. *Surf. Coat. Technol.* **1996**, *82*, 199–213.

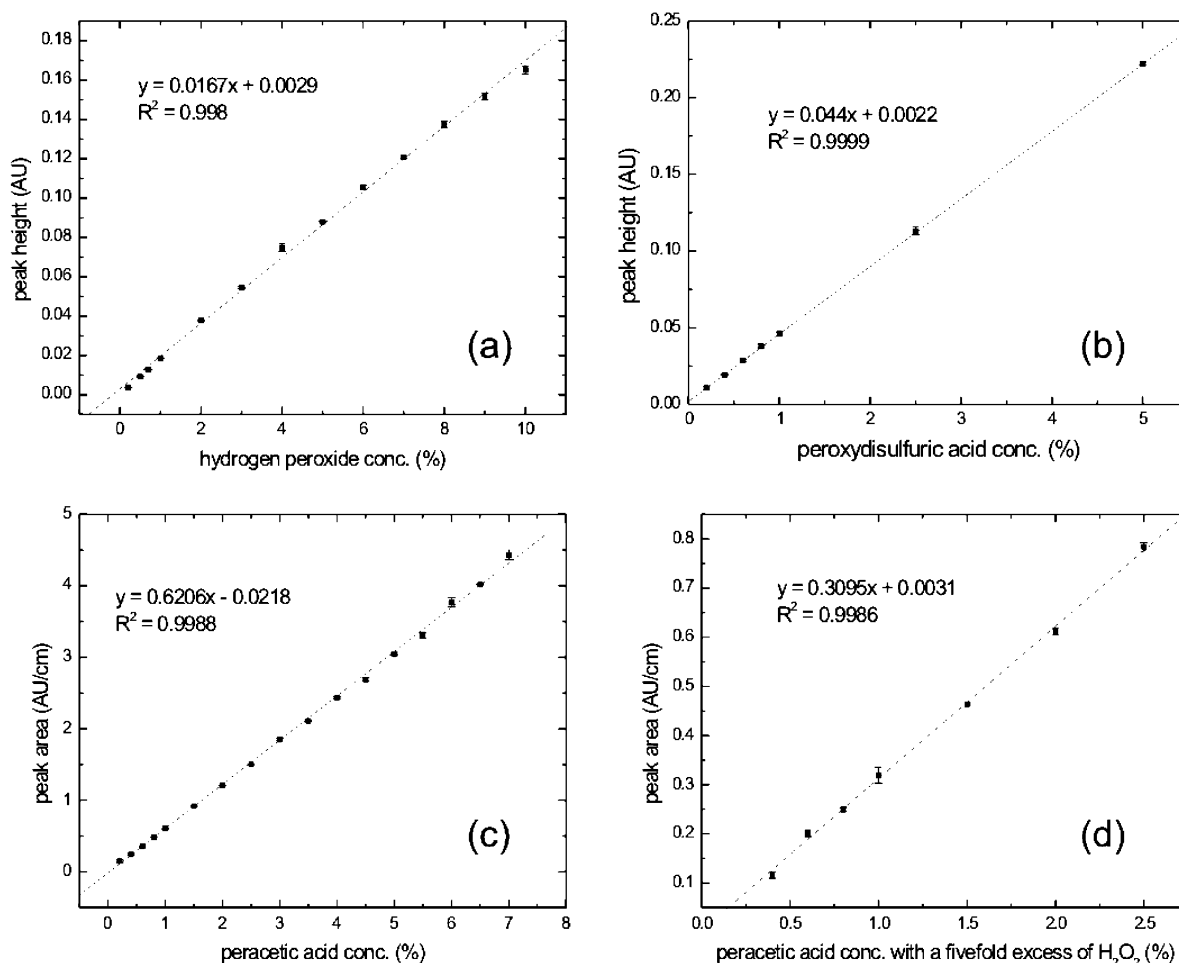


Figure 6. Calibration curves of hydrogen peroxide, peroxydisulfuric acid, and peracetic acid (evaluating δ (O–H) for H_2O_2 at 1382 cm^{-1} , ν_{as} (O– SO_3^{2-}) for peroxydisulfuric acid at 1272 cm^{-1} , and δ (C–O–O–H) for peracetic acid at 1217 cm^{-1}).

including the O–H deformation vibration (H2) and all major vibrational modes of acetic acid (A1, A2, A3), the spectrum of peracetic acid shows two main peaks at 1758 cm^{-1} (P1) and 1217 cm^{-1} (P3). These shifted bands are caused by the electronegative peroxide group facilitating differentiation between the two organic acids. The corded areas in the spectra indicate the absorption bands used for quantification of the ATR measurements by calculating either the peak height or peak area during nonchemometric data evaluation of individual compounds. Figure 6 demonstrates the correlation between the concentration of oxidizing agents and peak height or peak area, respectively, evaluating (a) δ (O–H) for H_2O_2 at 1382 cm^{-1} , (b) ν_{as} (O– SO_3^{2-}) for peroxydisulfuric acid at 1272 cm^{-1} , and (c) δ (C–O–O–H) for peracetic acid at 1217 cm^{-1} . Multiple analyte concentrations in a range from 0.2% up to 10% were consecutively detected three times, additionally providing the mean and standard deviation of the repeated measurements (Figure 6). The quality of the linear fit is given by the correlation coefficient and shows excellent linear behavior for all investigated oxidants with relative standard deviations generally $<2.5\%$ for each individual concentration value. Only data recorded for 0.2 and 0.4% concentrations result in relative standard deviations up to 10% as these values are close to the limit of detection (LOD) of the applied direct measurement technique. From the initial slope of the calibration functions and the standard deviation of blank measurements (deionized water),

the following LODs were determined for each analyte with DLC surface protected (100 nm) ZnSe ATR crystals: (i) 0.07% for H_2O_2 , (ii) 0.05% for peracetic acid, and (iii) 0.01% for peroxydisulfuric acid. In addition, a linear relationship between the peracetic acid concentration and the evaluated peak area is shown in the presence of a 5-fold excess of hydrogen peroxide (Figure 6d). These results verify that a calibration for PAA can also be carried out considering a large excess of hydrogen peroxide.

To characterize the measurement setup for dynamic operation, continuous measurements were simulated by pumping hydrogen peroxide solution with varying concentration levels from 1 to 5% through the ATR flow cell without recording new background spectra prior to concentration changes. The sensor response time to increasing and decreasing concentration changes and to the absence of analyte is evaluated and presented in Figure 7. The obtained results clearly illustrate that the sensor detects concentration changes of hydrogen peroxide with a response time of less than 1 min. Furthermore, the sensor gives the baseline response if no analyte is present. Due to the absence of an enrichment layer, the response time is predominantly influenced by the flow cell design and the FT-IR measurement parameters, such as spectral resolution and number of averaged scans. Recently, modeling to optimize ATR flow cell design and mass transport in the flow cell was discussed by our research group.⁴⁴ It has been shown that diffusion and advection resistance in the aqueous phase are the

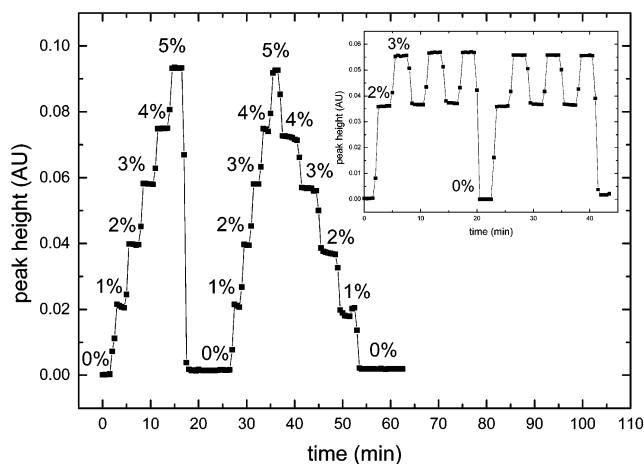


Figure 7. Continuous sensor response to increasing and decreasing concentrations of hydrogen peroxide. Graph in upper right corner shows continuous sensor response to 2 and 3% of hydrogen peroxide including two water purging steps.

rate-controlling parameters for the response time of the sensor. Minimization of these parameters can be accomplished by optimizing the sensor flow cell design. Concurrently adapting the FT-IR measurement parameters will yield effective response times significantly shorter than 60 s. The inset in the upper corner of Figure 7 demonstrates reversibility and repeatability of the applied on-line detection method as the standard deviation only varies between 1.14 and 1.23%.

As mentioned earlier, peracetic acid is only stable in the presence of H_2O_2 and acetic acid. Hence, for thorough analysis of peracetic acid samples using the developed IR-ATR technique with DLC surface protected waveguides, strongly overlapping spectral features of these compounds have to be taken into account (Figure 5). Chemometric data evaluation techniques were applied for improved data handling. PCR^{36–38} was selected as a viable approach for multivariate concentration evaluation of aqueous mixtures simultaneously containing peracetic acid, H_2O_2 , and acetic acid. Since PCR is based on multivariate least-squares regression,⁴⁵ instead of individual frequencies, all information contained in a measured spectrum is evaluated by determining the concentration values of the calibrated analytes.

The wavenumber region from 3000 to 1000 cm^{-1} containing 1556 measurement points has been used for PCR data evaluation. The calibration set totaled 40 samples: 4 acetic acid samples (2×2.5 and 2×7.5 vol % dissolved in water), 16 H_2O_2 samples (4 of each 0.5, 2, 5, and 8% dissolved in water), and 20 peracetic acid samples (4 of each 0.4, 1, 2.5, 4, and 6.5% dissolved in water). As mentioned above, the latter samples also contained 0.50, 1.24, 3.11, 4.97, and 8.07% acetic acid and 0.06, 0.15, 0.38, 0.60, and 0.98% H_2O_2 . These acetic acid and H_2O_2 reference concentrations and the calibration concentrations were determined by assuming the following concentrations in the stock solution: 32.2% peracetic acid, 4.83% H_2O_2 (determined by the titration method of Greenspan⁴⁶), and 40% acetic acid (according to the bottle label

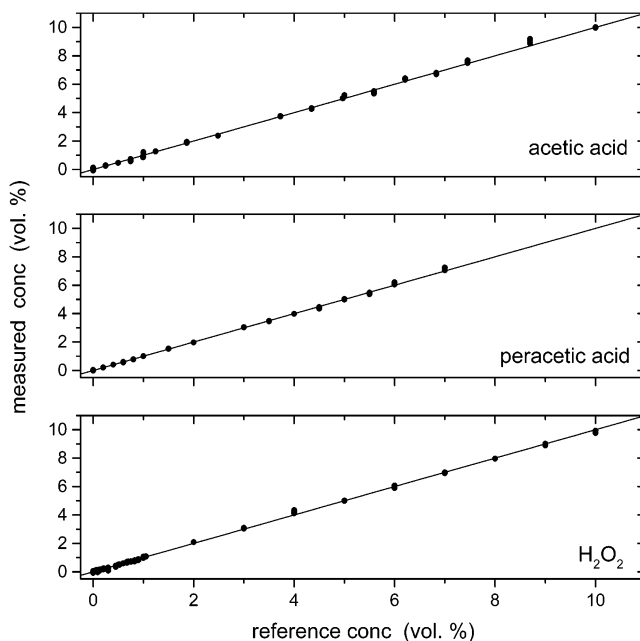


Figure 8. Concentration results for 148 test samples obtained by PCR. The straight lines indicate where the calculated results equal the reference concentrations.

of Sigma Aldrich). During calibration, a cross-validation³⁷ was performed in order to obtain PRESS values (predicted residual error sum of squares): PRESS (acetic acid) = 5.34×10^{-4} (vol %) (vol %), i.e., the estimated uncertainty based on PRESS is 0.023 vol %; PRESS (H_2O_2) = 1.01×10^{-4} (vol %) (vol %), i.e., the estimated uncertainty based on PRESS is 0.010 vol %; PRESS (peracetic acid) = 0.55×10^{-4} (vol %) (vol %), i.e., the estimated uncertainty based on PRESS is 0.007 vol %. After this PCR calibration, the remaining 148 samples were evaluated to simultaneously determine their peracetic acid, acetic acid, and H_2O_2 content and to assess the calibration model. In Figure 8 the PCR results of all three compounds are plotted versus the reference concentrations. As can be seen from Figure 8, all measured concentrations are in very good agreement with the input values.

CONCLUSION

We present a novel approach using DLC films as protective coatings on ZnSe ATR crystals for direct analysis of strongly oxidizing agents in aqueous solution. PLD allows the formation of thin DLC films (<100 nm) yielding a new generation of mid-IR waveguides with excellent mechanical and chemical stability. Detection of various oxidizing agents, such as hydrogen peroxide, peracetic acid, and peroxydisulfuric acid, and application of chemometric algorithms for multicomponent evaluation demonstrate the potential of surface-modified mid-IR optical sensors for on-line monitoring at harsh industrial conditions. By combining the dynamic sensor response results with the chemometric evaluation approach (see Figures 7 and 8), it is possible to simultaneously determine hydrogen peroxide and peracetic acid concentration and to continuously monitor their concentration profiles on-line. Due to the achieved sensor performance and the high stability of the DLC membranes, the developed system is a versatile alternative to currently existing methods for online detection of strongly oxidizing agents.

(44) Phillips, C.; Jakusch, M.; Steiner, H.; Mizaikoff, B.; Fedorov, A. G. *Anal. Chem.* **2003**, *75*, 1106–1115.

(45) Draper, N.; Smith, H. *Applied Regression Analysis*, 3rd ed.; John Wiley & Sons: New York, 1998.

(46) Greenspan, F. P.; MacKellar, D. G. *Anal. Chem.* **1948**, *20*, 1061–1063.

Hence, new opportunities for accurate analysis of wastewater, sterilization baths, or bleaching processes can be envisaged, e.g., the determination of hydrogen peroxide in cellulose fiber or paper bleaching baths.⁴⁷ In addition, chemometric algorithms proved valuable for precise data evaluation in such complex matrixes. Since on-line measurement techniques are a challenging task for spectroscopic data evaluation, extended algorithms are currently in development, which allow for dynamic adjustment of background drifts and correction of interfering uncalibrated spectral features.⁴⁸ These augmented algorithms are expected to play a major role in future applications of spectroscopic sensing with chemometric data analysis in process control.

(47) Vorarberger, H.; Ribitsch, V.; Janotta, M.; Mizaikoff, B. *Appl. Spectrosc.* **2003**, 57, 574–579.

(48) Vogt, F.; Mizaikoff, B. *Anal. Chem.* **2003**, 75, 3050–3058.

ACKNOWLEDGMENT

M.J., F.V., and B.M. acknowledge support by the U.S. Department of Energy (DE-FC26-00 NT 40920) and the U.S. Geological Survey within the National Water Quality Assessment Program (NAWQA). H.S.V., W.W., J.M.L., C.S., and M.B. acknowledge support by the Austrian Federal Ministry of Traffic, Innovation and Technology, the Austrian Industrial Research Promotion Fund (FFF), the Government of Styria, and the European Union. The authors are grateful to M.H. Wong (The Hong Kong Polytechnic University, China) for preparing the coated ATR samples at Laser Center Leoben.

Received for review June 26, 2003. Accepted October 8, 2003.

AC034699D